

Molecular Orbital Theory for Catalysis. Structures, Energy Levels, and Reactions of Acetylene with $Ni_2(COD)_2(RC\equiv CR)$, $Ni_2(C_5H_5)_2(RC\equiv CR)$, and the Ni(111) Surface

Alfred B. Anderson

Contribution from the Chemistry Department, Yale University,
New Haven, Connecticut 06520, and Chemistry Department, University of California,
Santa Barbara, California 93106.† Received April 29, 1977

Abstract: A molecular orbital theory combining two-body atomic repulsion and one-electron molecular orbital delocalization energies is used to examine catalytic reactions of acetylene on the Ni(111) surface and in di-Ni complexes. On the surface the theory shows that a high coordination adsorption site is preferred, unless complications such as acetylene-induced activated surface demagnetization play a role. By back-bonding into the acetylene π^* orbitals, the Ni surface causes a carbon bond elongation of 0.1–0.2 Å and an HCC angle bend of about 50° in the high coordination μ , di- σ , μ/π , and triangular sites. The carbon bond scission energy is reduced to about 25 kcal/mol, while at coverages greater than quarter monolayer the spontaneous dissociation into CH fragments observed by Demuth indicates that steric factors cause a coupling of released adsorption energy to the bond scission mode. Despite distortions, energy levels for chemisorbed acetylene are close to those in the free molecule. In particular, the $s\sigma_g$ C–C orbital is stabilized by a nonbonding type of mixing with Ni 4s and 4p orbitals. Converging results on going from Ni_4 to Ni_{31} surface models are obtained. In the $Ni_2(COD)_2(RC\equiv CR)$ and $Ni_2(C_5H_5)_2(RC\equiv CR)$ complexes, antibonding interactions with ligand π orbitals squeeze the $Ni_2 s\sigma_g$ bonding orbital up to a high energy, emptying it into the Ni_2 d band, reducing the bond order to zero in the COD complex. As acceptors, the two C_5H_5 ligands drain two electrons from the top of the Ni_2 band of energy levels, resulting in a bond order of one. The ability of the COD complex to react at 20 °C with hydrogen and with hydrogen plus $RC\equiv CR$ to form stoichiometrically and catalytically >95% cis alkene as observed by Muetterties and co-workers is made possible by the Ni–Ni bond weakness. The Ni_2 bond length and acetylene distortions in $Ni_2(C_5H_5)_2C_2H_2$ are calculated, agreeing accurately with experiment.

I. Introduction

Theory shows considerable promise for allowing the determination of molecular structures, energy levels, and reaction pathways in coordination compounds, on single crystal surfaces, films, and clusters. By the same token, theory will play a role in the development of our understanding of heterogeneous and homogeneous catalytic processes.

In surface chemistry little is known of actual overlayer atomic and molecular binding sites and structures. Low-energy electron diffraction studies have given us the binding site and surface to overlayer distance for a few cases such as O, S, Se, and Te on Ni(100),¹ O on Fe(100),² N on Cu(100),³ and acetylene on Pt(111).⁴ By saturating Pd films with deuterium it has been inferred that 1,3-sigmatropic shifts catalyzed by the film are intramolecular.⁵ However, the list of examples of where it is known positively what is happening structurally on surfaces dwindles.

When surface structures and bond lengths are unknown, Mulliken–Walsh⁶ analyses are often impossible, even when sensible, for they are used to understand angular preferences in structures where bond lengths are constant. The problem on surfaces is one of bonding site and adsorbate distortions, not one of angular or rotational conformation, at least as yet.

Most theoretical efforts to date have assumed model geometries and then examined orbital overlaps between the surface and adsorbate and shifts in adsorbate electron energy levels to compare with shifts seen in photoemission spectra. Frequently very small clusters of atoms are used to represent the surface, as in extended Hückel⁷ studies of interactions of small molecules with transition metals, CNDO studies,⁸ or the extreme NiO_6^{10-} model used to represent surface Ni oxides in an $X\alpha$ study.⁷ In each case orbital overlaps and concomitant orbital energy shifts are qualitatively sensible. A model extended Hückel calculation has shown that the above 1,3-sigmatropic shift is catalyzed by surface metal atom d orbital

stabilization of the π orbital in the transition state.¹⁰ All of these model calculations are of interpretative value but predict little. What is needed is an efficient and tractable procedure for calculating structures of adsorbates on large clusters representing surfaces.

In the case of cluster complexes, for which many x-ray structures are available, analyses in the Mulliken–Walsh sense are possible, and numerous molecular orbital analyses appear throughout the inorganic literature. Still, there is something to be gained even in inorganic bonding analyses if theory is able to produce bond lengths and reaction energy surfaces.

The purpose of this paper is to outline a molecular orbital theory designed for problems in inorganic and surface chemistry. Subsequently a discussion of two catalytic reactions follows, one involving acetylene carbon bond scission on the Ni(111) surface and the other hydrogenation by a dinickel complex.

II. Theory

The theory is a two-step process.¹¹ First, atoms are superimposed and the interaction energy is calculated; and, secondly, electron delocalization is turned on and the delocalization energy is estimated. These components are summed, producing an approximate molecular energy.

The exact charge density distribution in a diatomic molecule a–b may be written as the sum of atomic charge densities ρ_a and ρ_b , and the non-perfectly-following contribution making the total equal to the exact molecular density. These components are shown schematically in Figure 1. On integrating the Hellmann–Feynman¹² electrostatic force on one of the nuclei, two formally exact energy components, a repulsive one, E_R , due to superposition of the rigid atoms and an attractive one, E_{NPF} , due to electron delocalization and charge redistribution, are obtained, as shown in Figure 2. It happens that the repulsive component contains stretching force constants, and higher order ones by taking derivatives, as shown in Figure 3. It can

† Present address.

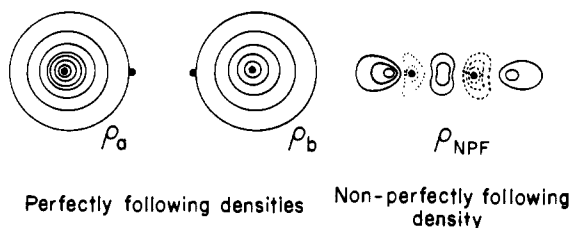


Figure 1. Schematic representation of perfectly following atomic charge densities ρ_a and ρ_b and the non-perfectly-following relaxation density, ρ_{NPF} .

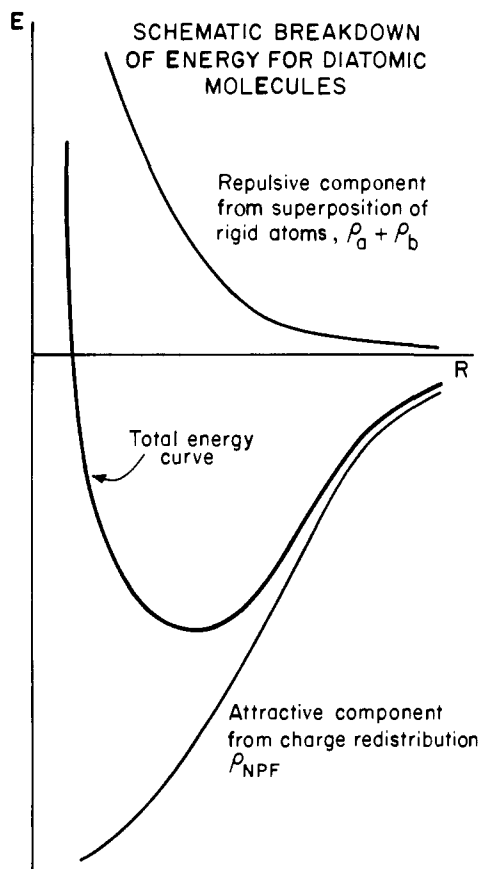


Figure 2. Schematic representation of the attractive and repulsive energies from integrating the Hellmann-Feynman forces due to charges in Figure 1.

be shown that insofar as this Poisson equation works, the Laplacian of E_{NPF} is zero.¹³

The repulsive component, E_R , is given as¹¹

$$E_R = \sum_{a < b} -Z_b \int \rho_a(\mathbf{r})(\mathbf{R}_b - \mathbf{r})^{-1} d\mathbf{r} \quad (1)$$

where Z is a nuclear charge and ρ includes the nuclear charge. The attractive component, however, can be calculated from a similar formula only if we know the R dependence of ρ_{NPF} . Unfortunately, ρ_{NPF} is not given and is only a result of exact quantum mechanical calculations.

To estimate E_{NPF} the superimposed rigid atom model is retained and the atomic Fock potentials, those for which single-determinant one-electron self-consistent field atomic orbitals are the eigenfunctions, are superimposed.¹¹ A linear combination of atomic orbitals molecular-orbital wave function is used to diagonalize this Hamiltonian with three approximations. First, electron affinities are assumed to be smaller than atomic valence ionization energies. Second, orbitals in two-center integrals are expanded about a single center and

Figure 3 shows a diagram of a charge density ρ_a with a point R_e on its surface. An arrow points from the text below to this point. The text defines the force constant k_e as the second derivative of energy with respect to distance at R_e .

CLASSICAL ELECTROSTATIC POISSON EQUATION - Follows quantum mechanically from the Hellmann-Feynman approximation for the model $\rho = \rho_a + \rho_b$. Exact if $\nabla^2 E_{NPF} = 0$ i.e. $E_{NPF} \sim C/R$ near R_e .

Figure 3. Depiction of the Poisson equation for force constants.

the first nonzero term is retained. Third, an inverse radial form is assumed for the atomic Fock potentials, allowing some two-center integrals to be put into orbital ionization energies via the virial theorem. The result is the extended Hückel Hamiltonian,¹⁴ eigenvalues and molecular orbitals. This derivation of the extended Hückel theory also shows what the method omits, namely, E_R . The derivation shows that the delocalization energy E_{NPF} is to be approximated by a semiempirical one-electron molecular orbital energy. In practice, this more general theory damps the extended Hückel off-diagonal matrix elements by an exponential distance damping factor.¹¹ Thus we have for the total energy E

$$E = E_R + E_{NPF} \approx E_R + \text{modified extended Hückel energy} \quad (2)$$

This equation can yield estimates of molecular structures, force constants, and relative binding energies for large, as well as small, systems. Since experimental atomic valence state ionization energies are employed in the orbital determination of E_{NPF} , the molecular orbital energy levels contain atomic relaxation shifts¹⁵ and compare favorably with experimental photoemission spectra.

The above theory has been used to study numerous systems which are referenced and can be found in references to follow. In many of these, literature Slater exponents¹⁶ and atomic ionization energies¹⁷ are employed. However, recent examinations of Ni and Fe(100) surface oxides show that atomic ionization energy shifts, to counteract excessive charge transfer, and spin unpairing in the d band are important.¹⁸ This paper tests their effect by comparison to an earlier study where they were ignored.¹⁹ Parameters used are in Table I.

An examination of diatomic results in papers referenced shows that bond lengths and force constants are usually calculated within a few percent of experiment and bond energies within 50%. It is impossible to address the accuracy of the theory in an absolute sense. Adjustments in valence state ionization energies due to uncertainties in their experimental estimation or in Slater orbitals can improve these quantities, but since electron interaction energies of the types omitted, such as ionic contributions, can affect results, the parameters should not be overadjusted. This effect no doubt plays a role in the bond energies being calculated about one-third low for NiO and FeO. It is significant that the atomic parameters are transferable among dissimilar molecules such as Fe₂, O₂, and FeO, modified by the demands of self-consistency.

III. Ni₂(C₅H₅)₂(RC≡CR) and Ni₂(COD)₂(RC≡CR)

A revealing test of the theory and its ability to treat acetylene-Ni μ bonding involves calculating the structure of Ni₂(C₅H₅)₂C₂H₂ and comparing with a recent x-ray structural determination.²⁰ As shown in Figure 4, when the Ni₂(C₅H₅)₂ structure is fixed to experiment, the calculations produce an

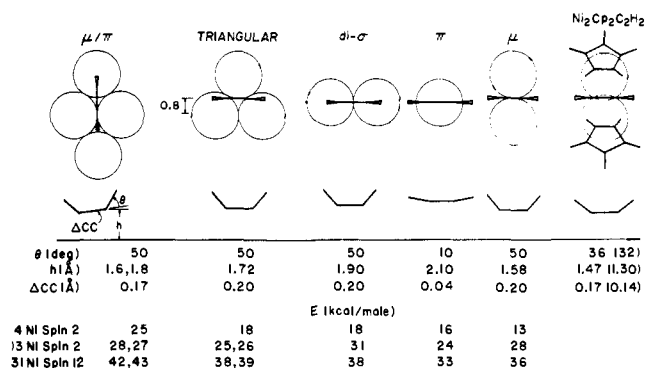


Figure 4. Acetylene binding sites on Ni(111). Calculated structures are based on a diamond-shaped Ni_4 cluster. When two energies are given, the first is for a high coordination site without an atom beneath in the next monolayer. Experimental $Ni_2CP_2C_2H_2$ acetylene geometry indicated in parentheses is from ref 20; other atoms are put in the experimental site for the calculations on acetylene.

Table I. Parameters Used in the Calculations, Not Including Ionization Energy Shifts Discussed in the Text

Atom	Principal quantum no.			Slater exponent			Ionization energy, eV		
	s	p	d	s	p	d			
Ni ^a	4	1.8	7.635	4	1.5	3.99	3	5.75 ^b	10
C ^c	2	1.658	20.0	2	1.618	11.26			
H ^c	1	1.2	13.6						

^a From ref 19 and 25. ^b The second exponent in the double ζ function is 2.0 and the respective coefficients are 0.5683 and 0.6292. ^c From ref 19.

acetylene structure within a few degrees and a few hundredths of an angstrom of experiment. Further calculations show that the Ni-Ni bond wants to stretch about 0.1 Å if the cyclopentadienyl ligands follow. The calculated Ni-Ni bond order is about 1, consistent with the 2.33-Å length.

In these calculations the C and H atomic valence ionization energies are decreased 1.0 eV and those for Ni increased 1.0 eV, following ref 18, to reduce charge transfer to acetylene carbon atoms to about 0.4 electron. Shifts of this magnitude are clear for oxygen on Ni and Fe surfaces according to photoemission spectra for Ni(111)²¹ and Fe(100)²² and as analyzed in ref 18. Thus they are likely for hydrocarbon adsorbates, although coverages are low enough that shifted metal ion levels due to surface atoms do not make a noticeable contribution to the photoemission spectra, as most photoelectrons originate from several layers of bulk metal atoms beneath the surface. Without the ionization energy shift, the Ni-Ni bond length is infinite in the calculations, though when the Ni(C₅H₅) units are fixed at experimental geometries, the acetylene distortions are practically unchanged. An accurate μ -acetylene geometry has also been calculated using the theory on Fe₂(CO)₆C₂H₂²³ according to comparison with an x-ray structure for Fe₂(CO)₆(*t*-Bu)₂C₂.²⁴ Here theory verifies the suggestion in ref 24 that the Fe-Fe bond order is 2. For the iron complex atomic ionization energy shifts were not made. Thus it seems that in these bimetallic complexes ligand geometries are less sensitive to atomic and molecular orbital energy level shifts caused by charge transfer than are metal bond strengths, as the Fe-Fe bond was also unstable without shifts.

The μ -acetylene complexes $Ni_2(CP)_2(PhC\equiv CPh)_2$ (CP = C₅H₅ and Ph = C₆H₅) and $Ni_2(COD)_2(RC\equiv CR)$ present an interesting contrast since the former is not a hydrogenation catalyst, while the latter is. Two reactions are observed for the COD complex at 20 °C. Hydrogen reacts stoichiometrically

yielding 95% cis alkene, as does hydrogen plus $RC\equiv CR$.²⁵ The long Ni-Ni bond in the COD complex and sterically free region opposite the acetylene would appear to play a role, as discussed in ref 25. Indeed the Ni-Ni bond weakness allows a monomer-dimer equilibrium and acetylene ligand lability: $Ni_2(COD)_2(RC\equiv CR) + RC\equiv CR = 2Ni(COD)(RC\equiv CR)$. As discussed in ref 25, hydrogen probably adds to the Ni₂ region of the dimer as the first step toward cis hydrogenation.

In the following calculations, acetylene substituents are replaced by hydrogen atoms and each COD ligand by two ethylene molecules. CH bond lengths are taken to be 1.1 Å and otherwise experimental geometries are used. These computational simplifications do not affect the important metal-ligand interactions.

The Ni₂ molecule is a suitable starting point for discussing the complexes. Ground-state Ni atoms have the 3d⁸4s² configuration. The bonding of two or more atoms in a cluster correlates best with d⁹s¹ Ni atoms almost to the dissociation limit. This is because at bonding distances the $s\sigma_u$ orbital is high in energy and will donate its two electrons to the d band. These and other features of Ni cluster bonds are discussed and compared with experimental optical data elsewhere.²⁶ The same thing will happen in CP and COD acetylene Ni₂ complexes when we imagine beginning with Ni₂ and then introducing the ligands. The d⁹s¹ assignment is important only to the Ni two-body repulsion energy (as 3d electrons shield the nucleus more completely than 4s electrons) and does not affect the molecular orbitals in any way. With the configuration $s\sigma_g^2d\pi_u^4d\sigma_g^2d\delta_g^4d\delta_u^4d\sigma_u^2d\pi_g^2$, Ni₂ has a bond order of 2 and a calculated bond length of 2.21 Å.² The $s\sigma_g$ orbital is the strongest contribution to the binding energy owing to its diffuseness and consequent large overlap and stabilization.

The ligands severely perturb certain Ni₂ orbitals and their energy level placements. First, the $s\sigma_g$ orbital is pushed up out of the binding picture to 3.56 eV in the COD complex and 6.61 eV in the CP complex. Thus a whole bond is formally lost. Small $s\sigma_g$ and $s\sigma_u$ hybridization mixing occurs in ligand, metal, and ligand-metal orbitals, but is of no consequence. The pushing up of the $s\sigma_g$ level is a result of antibonding interactions with the ligand π systems. A similar shift occurs for Ni atomic 4s levels in Ar matrices owing to interactions with the filled Ar p orbitals, but is only a few tenths of an eV because Ni-Ar distances are much longer than Ni-ligand distances.²⁶ This general phenomenon is likely to occur elsewhere, the shift being greatest in coordination and cluster complexes.

Other Ni₂ levels are less perturbed owing to rehybridization from bonding with the ligands. Figure 5 shows all the filled energy levels for the complexes, including the Ni₂ d band with the expected ten levels. For the CP complex four additional Ni-Ni nonbonding levels enter the d band, showing metal-CP orbital mixing and bonding. Denoted in Figure 5 are the acetylene levels and the Ni₂ + acetylene π bonding interactions. Lower acetylene σ framework molecular orbitals mix only slightly with Ni₂. The lowest $s\sigma$ acetylene, CP, and COD framework levels are stabilized several tenths of an eV as the result of antibonding interactions with the Ni 4p orbitals. This is responsible for the shifting of the acetylene $s\sigma$ level back to nearly its original position in the free molecule. Otherwise, HCC bending and CC stretching would have raised the level about 0.5 eV, as discussed later.

The d band region of the two complexes are shown in greater detail in Figure 6. The CP complex d band is wider because the Ni-Ni distance is less. In it all Ni₂ levels are accounted for except a δ_g and δ_u set. These must correlate with the two unsymmetric nonbonding orbitals. Most orbitals are quite severely rehybridized by ligand interactions, making symmetry assignments rough. Noting the loss of the $s\sigma_g$ orbital and the fact that the highest d band level is empty, we see that the Ni-Ni bond order is formally 1 and hence the length is 2.33

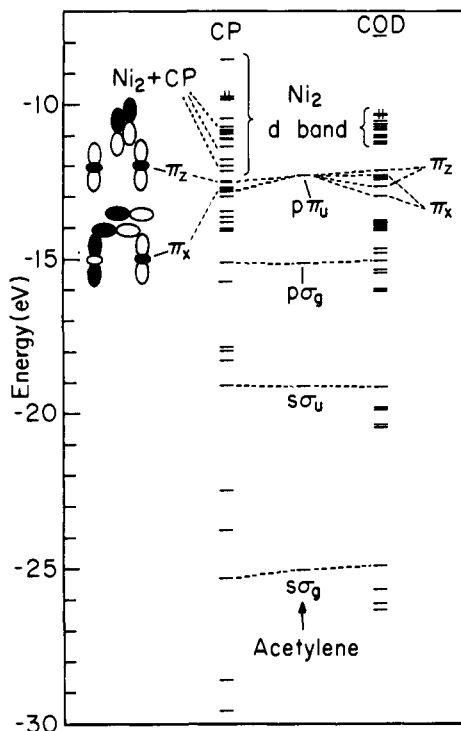


Figure 5. Energy levels for the CP and COD complexes. Free acetylene levels, based on unshifted (see text) C and H valence ionization energies, are shown for comparison. The CP complex structure is taken from O. S. Mills and B. W. Shaw, *J. Organomet. Chem.*, **11**, 595 (1968), and the other from V. W. Day, S. Abdel-Mequid, S. Dabestani, M. G. Thomas, W. R. Pretzer, and E. L. Muettteries, *J. Am. Chem. Soc.*, **98**, 8289 (1976). Ligand simplifications in the calculations are outlined in the text.

Å, appropriately longer than 2.21 Å, for double-bonded Ni₂.²⁶ Based on Ni₂ charges in these orbitals the bond order is 0.49. Contributions from lower orbitals are small. Addition of the metal-acetylene π -bonding contributions brings the charge bond order to 0.57, still small. The bridging acetylene itself may help hold the complex together. This will be evident in a consideration of the COD complex.

The highest lying Ni₂ antibonding orbital is empty in the CP complex because each CP is an acceptor with a half-filled p orbital. In the COD complex there are no partially filled acceptor orbitals, and so the Ni₂ d band is filled, as in Figure 6, and the bond order is formally 0, hence the long 2.62 Å bond. The charge density bond order is -0.08. Why are the Ni atoms together at all? The answer lies in the bridging acetylene. Four Ni₂-acetylene π -bonding orbitals result in a charge density bond order of -0.11 when added to d bond contributions. This means that the Ni₂-acetylene bonds are holding this complex together.

With this analysis the extra long bond in the COD complex is understandable. The consequent open structure around Ni₂ opposite the acetylene molecule allows access by H₂, which forms cis-hydrogenated acetylene, as discussed experimentally in ref 25.

IV. Bulk and Surface Nickel

The photoemission spectra of Ni(111) and other surfaces appear in several places in the literature, usually showing a single-peaked band,²¹ but some spectra,²⁷ presumably of higher resolution, show a double peak in the range 1-2 eV beneath the Fermi energy, as shown in Figure 7. Also present is an interesting bump centered at 6 eV in Figure 7, a feature missing in many such spectra, and lying in the area of 0 and its first excited multiplet as may be seen in ref 18, though Auger measurements do not disclose any 0 on the surface.²⁷

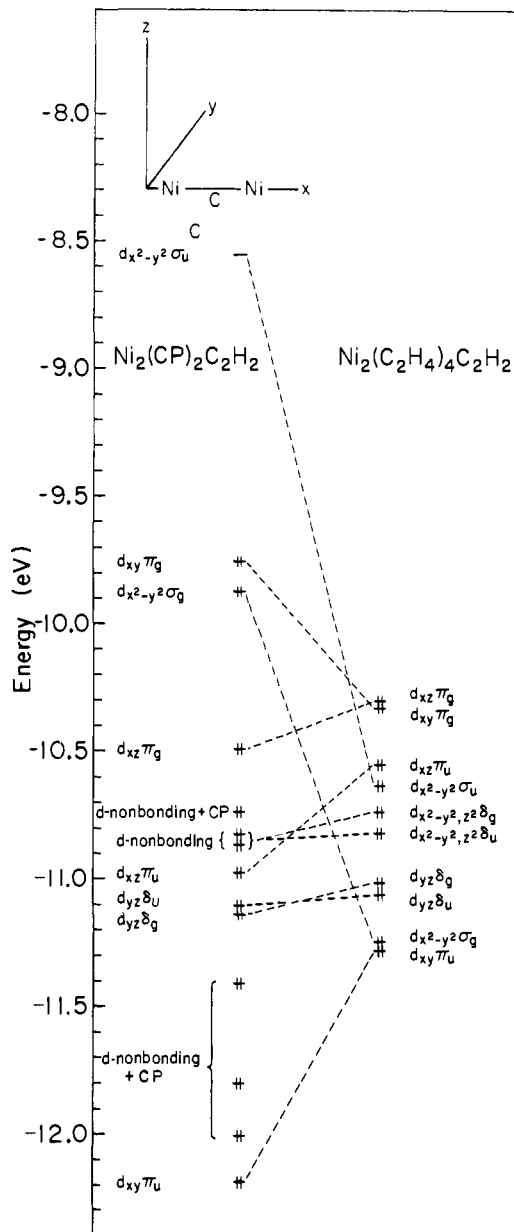


Figure 6. Close-up of the Ni₂ d-band levels in Figure 5.

Calculations on a Ni₁₃ fcc cluster with bulk bond lengths 2.48 Å produce a band of energy levels 2 eV wide. The ones whose molecular orbitals are strongly associated with the fully coordinated central atom are shown in Figure 7. A split bonding and antibonding set of t_{2g} and e_g levels is visible. Since the doublet in the spectrum is 1 eV wide, the 1.8-eV calculated splitting is a possible cause. Larger clusters will add levels throughout the d band. The Ni₃₁ cluster (Figure 8) produces just such a result. It will be necessary, however, to use much larger clusters for each atom to be in a bulk environment; the N₃₁ atom cluster is only two layers thick and has no completely coordinated atoms. There is no significant dependence of the measured spectrum on crystal face chosen,²⁷ though such a dependence exists for some materials, including Ir.²⁸ Electrons from many bulk atoms contribute to the spectrum. If the surface is a relatively small perturbation to these bulk atoms, better agreement may be expected for the Ni₁₃ central atoms in Figure 7, representing the bulk, than for the Ni₃₁ slab, representing the surface.

If the broad feature in the spectrum is due to Ni, it is possibly associated with the 4s band. Such a result would favor using

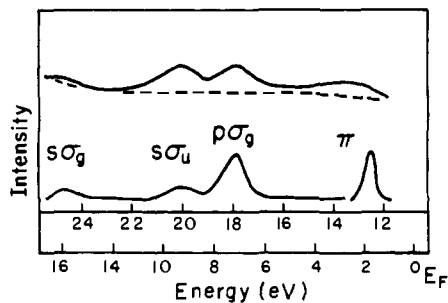


Figure 7. Photoemission spectrum from ref 27. Levels corresponding to large central atom molecular orbital contributions in the fcc Ni_{13} cluster are shown, as is the filled s-d band for Ni_{31} (Figure 6).

atomic Ni parameters from ref 26. In such a case the shifts in atomic ionization energies for chemisorption would change. On the other hand, this feature may be an electron shake-up or plasma oscillation.

The spin per atom on occupying each d band level with at least one electron is 0.5, 0.46, and $0.39 \mu_B$ for the 4, 13, and 31 Ni atom clusters (Figure 6), respectively. Though not as large as $0.6 \mu_B$ for bulk Ni,²⁹ this is close and, by this rule, the spin is sensitive to the relative placements of the 3d and overlapping 4s band. If the feature in the photoemission spectrum in Figure 7 is due to the 4s band, then the spin per atom by the unpairing rule will be $1-2 \mu_B$, which is large. Finally, the spin per atom of the fcc Ni_{13} cluster is $0.62 \mu_B$, probably accidentally close.

V. Chemisorbed Acetylene

One of the purposes of this study is to examine the effects of larger clusters on relative binding energies and molecular orbital energy level shifts for acetylene. Once the acetylene structure is determined for a particular binding site on a Ni_4 cluster, this geometry is used for the larger clusters as well. A test of the validity of this program for acetylene bonded in a triangular site on Ni_{13} shows that the same structure is energetically preferred as on Ni_4 within 5° for the CCH angle, within 0.02 \AA for the C-C bond length, and within 0.1 \AA for the placement of the C-C axis. This means that the surface-adsorbate bond is localized and that the adsorbate dominates surface metal hybridization, not neighboring metal atoms. This constancy might not hold for the total binding energy, however. The balance of the two-body repulsion energy E_R against electron delocalization energy E_{NPF} in producing geometries is independent of the magnitude of E_{NPF} . That is, structures depend on the slopes of these components of energy, the respective forces, which are local, and not on delocalized bulk polarization.

Calculations produce similar acetylene distortions for all sites but the one-fold π site, as is displayed in Figure 4. The C-C bond structures are about 0.2 \AA and the HCC bonds bend about 50° . These may be overestimated about 4° and 0.03 \AA as for the Ni_2 complex. In the π site the stretch is 0.04 \AA and the bend 10° . On the Ni_4 and Ni_{31} clusters the μ/π site is preferred by several kcal/mol over the others. There is no apparent preference between sites with a hole or an atom beneath in the second monolayer. The closeness of the calculated binding energies for the sites suggests that acetylene is readily mobile on the surface and that, at (2×2) coverage, any one could be preferred if acetylene interactions play a role. On Pt(111) there are two phases of (2×2) quarter monolayer coverage acetylene. The first is weakly held, displaced 0.25 \AA toward a hole with an atom beneath from the π site and 0.45 \AA further from the surface than the second phase. Heating converts to the second phase, which has acetylene molecules in a Δ site with a hole beneath in the second layer.³¹ While no

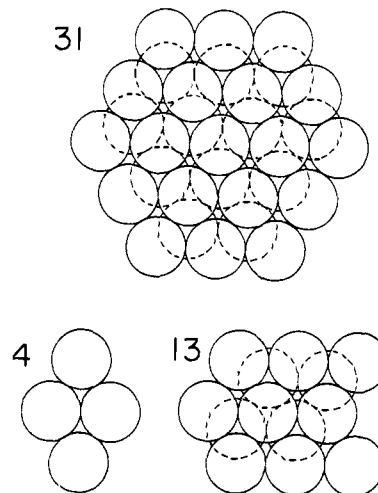


Figure 8. Models for the Ni(111) surface as used in the calculations. The nearest-neighbor internuclear distance is 2.48 \AA .

calculations have been performed for the Pt surface, the system is isoelectronic to Ni. Since low-energy electron diffraction beams dissociate chemisorbed acetylene on Ni,³¹ the structure has not been determined. If a parallel behavior for these systems is assumed, then the phase transformation lacks a simple explanation, according to the acetylene on Ni(111) calculations. Perhaps there is an activated spin pairing, or unpairing on the surface as acetylene goes from the π to Δ position on Pt. Molecular orbital theory will not provide elucidation concerning this possibility, but surface magnetism measurements might. On the other hand, molecular orbital structural calculations for the Pt system might be revealing. A model extended Hückel study implies a preference for high coordination sites.³²

Calculated binding energies in Figure 4 increase with cluster size to about $2/3$ of the 67 kcal/mol reported for adsorption on a polycrystalline film.³³ This calculated value depends on the approximation of constant atomic ionization energy shifts up to nearly the limit of dissociation from the surface. This is, of course, rough, but it has been argued that for ionic systems such as FeO it is not unreasonable.¹⁸ In earlier calculations without these shifts the adsorption energy was calculated to be much larger.¹⁹ The increasing binding energy with cluster size is a result of increased stabilization of acetylene levels as seen below, ionization energy shifts and spin being kept fixed.

Starting with acetylene in a triangular site, the barrier to C-C bond scission is calculated to be about 25 kcal/mol , doubled as a result of shifting atomic ionization energies. This is more consistent with the fact that acetylene is stable at temperatures up to 470 K in the (2×2) coverage.³⁴ However, recent photoemission spectra indicate that even at room temperature, acetylene in addition to the quarter monolayer (2×2) layer will adsorb and gives rise to what appears to be, on the basis of calculations in ref 19, CH fragments from dissociation.²⁷ Construction of a model easily shows that no matter where the molecules in the quarter monolayer sit, additional undissociated acetylene adsorption is sterically forbidden. However, if some of the released adsorption energy can couple to a C-C bond-breaking motion to make CH fragments, these fragments can bond to the surface. The fact that the (2×2) LEED pattern is destroyed on further adsorption²⁷ suggests that the incoming molecules push already adsorbed molecules aside while dissociating.

The calculations indicate that the CH fragments sit in threefold sites about 1.35 \AA above the surface. The C-H axis is perpendicular to the surface, C and down. This maintains strong σ and π C-Ni bonds. This orientation gives CH a small

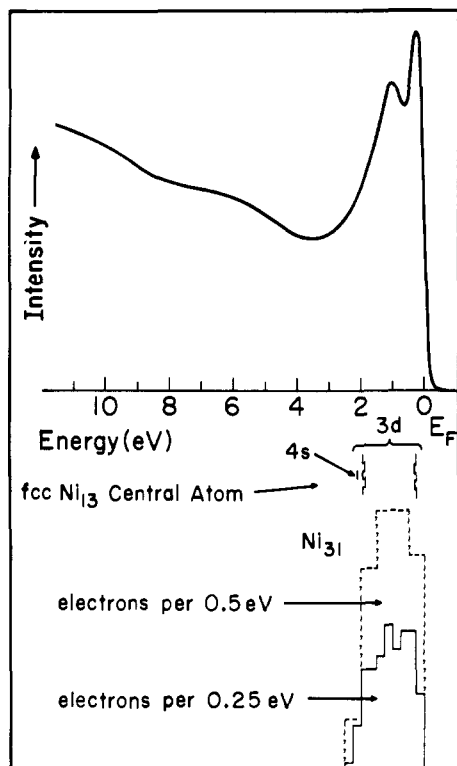


Figure 9. Photoemission spectrum for free acetylene and the difference spectra for acetylene chemisorbed on Ni(111) taken from ref 27.

surface van der Waals radius, allowing it to fit between acetylene molecules.

Photoemission spectra for free and chemisorbed acetylene appear in Figure 9. This 40.8 eV photospectrum shows²⁷ all of the valence molecular orbitals for acetylene, including the $s\sigma_g$ C-C bond, which is beneath the cutoff in the initial 21.2-eV photon study.³⁴ A shift of about 1.2 eV for the π levels is a consequence of bonding stabilization from π plus mixing with the bottom of the s-d bond. The σ -framework energy levels experience smaller shifts. Does this spectrum imply anything about surface structure?

Figure 10 shows energy levels for free and distorted acetylene with and without surface present. The σ -framework shifts are, with bonding, less than for Hartree-Fock calculations on acetylene,³⁵ but those calculations do not estimate relaxation shift corrections.³⁵ With a C-C bond stretch of 0.2 Å, $s\sigma_g$ and $s\sigma_u$ level shifts are about 0.5 eV. On the Ni_4 , Ni_{13} , and Ni_{31} surfaces the $s\sigma_g$ is progressively shifted back to a position 0.2 eV below that for free acetylene and thus $s\sigma_u$ level rises about 0.1 eV toward its starting value. The π levels are shifted down ~ 0.9 eV and spread about. This favors the shifts in C, H, and Ni ionization energies, for in the first study¹⁹ the acetylene π and Ni s-d bond were so separated that there was no significant shift in the acetylene π levels. At heavier coverage, with four acetylene molecules in π/u sites on a Ni_{16} cluster, the $s\sigma_g$ levels span 0.3 eV, the $s\sigma_u$ levels span 0.13 eV, the $p\sigma_g$ levels span 0.03 eV, and the π levels span 0.49 eV, counting $p\pi_g$ back-bonding orbitals. The π spread is visible in the spectrum.

Changes in energy level positions with adsorption site are slight. In Figure 10, the bond stretch for the di- σ site is only 0.1 eV, to test the effect of a smaller stretch should the calculations overestimate it. This puts the $s\sigma_g$ and $s\sigma_u$ levels only 0.4 and 0.1 eV beneath the gas-phase values, respectively, even though the HCC angle is 130°. Note that in the complex the σ levels are shifted only about 0.1 eV, despite the distortions in acetylene. These results strongly suggest that acetylene is distorted and rehybridized approximately to the degree calculated and contradict the analysis based on Hartree-Fock

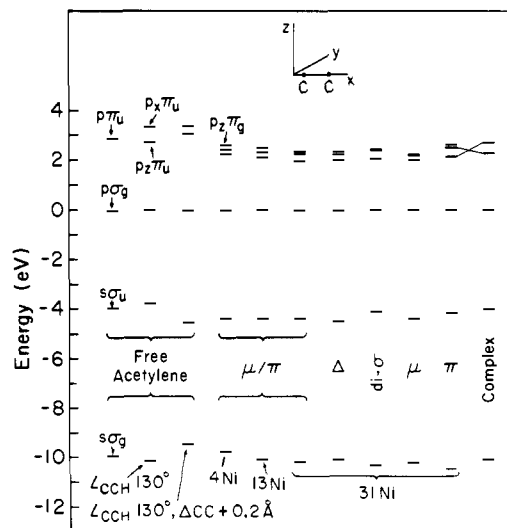


Figure 10. Calculated energy levels for free, stretched, bent, chemisorbed, and complexed acetylene as in Figure 4. The $p\sigma_g$ levels are aligned. For the di- σ position, $\Delta CC = 0.1$ Å.

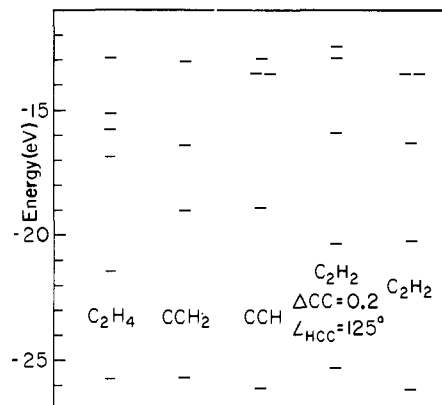


Figure 11. Calculated energy levels for free and distorted acetylene and CCH, CCH₂, and C₂H₄.

energy levels not corrected for relaxation effects, and not including surface Ni atoms. From that analysis, the small σ -framework perturbation in the photoemission spectra is taken to mean that acetylene distortion and rehybridization is less.³⁵ Of course, if the π site is actually the preferred one, then distortion and energy level shifts are indeed small, except for the lowest $s\sigma_g$ level. This level is stabilized by an interesting antibonding interaction^{19,36} with metal 4s and 4p orbitals. In the π position it may be stabilized too much to agree with the spectrum, though this effect, which depends on the diffuseness of Ni 4p orbitals, is not well understood, so that its correct magnitude is uncertain.

These calculations also do not support the view that distorted acetylene will produce an olefinic complex as suggested by interpretations of photoemission spectra.³⁷ This is because a C-H bond is not like a C-metal bond in determining electron energy levels. A hydrogenated or rearranged acetylene is a more probable cause of the loss of acetylene spectrum on Pt and Pd(111) as seen in ref 37. This could happen even without affecting the LEED structural analysis in ref 30. As none of the fragment energy levels in Figure 11 are a good match to ethylene, ethylene formation is favored by the calculations, although the possibility of a mixture of fragments cannot be discounted on the basis of these calculations.

VI. Conclusions

This molecular orbital study has shown and suggested several new things.

(a) The structure, including Ni–Ni bond order and acetylene distortions, is accounted for in $Ni_2(C_5H_5)_2C_2H_2$. Theory predicts that acetylene energy levels shift only a few tenths of an eV with respect to each other, despite acetylene distortions.

(b) Antibonding interactions with ligand π systems force the $Ni_2 s\sigma_g$ bonding orbital to a high energy, emptying it into the d band of levels. This reduces the bond order by one as the band is over half full. This is probably a common phenomenon.

(c) In the CP di-Ni complex half-filled carbon orbitals on the CP ligands drain two electrons from the d band, leaving a bond order of one. In the COD analogue there are no acceptor orbitals, so the bond order is zero and the nickel atoms are held together by the bridging acetylene. The long metal bond affords access by hydrogen and consequent cis hydrogenation.

(d) On Ni(111) acetylene is mobile at room temperature and below. Unless acetylene causes an activated magnetization or demagnetization of the Ni surface on going from a π to a high coordinate site, one of the latter is preferred.

(e) On Ni(111) the calculated energy level spectrum is close to that for free acetylene no matter which bonding site is chosen. Consequently, detailed structural information is not available in the photoemission spectra for acetylene, though variations in σ level shifts between metal surfaces have been noted and correlated with C–C bond stretches.²⁸

(f) Rehybridized acetylene bonded to metal atoms does not produce an olefinic set of energy levels, but rather a somewhat distorted acetylene set. Bonding interactions with the σ framework levels appear strongest for the lowest symmetric one, which is stabilized through a negative overlap with Ni 4s and 4p orbitals.

(g) Generally, Ni is less reactive toward acetylene than Fe, whose reactivity was predicted in an earlier study³⁸ and verified experimentally.³⁹ This is because Ni 3d orbitals are more compact.⁴⁰ Using Fe^+ d orbitals, which are nearly the same as Ni orbitals, the reactive ability of Fe is reduced so that a barrier similar to that on Ni(111) exists for C–C bond scission. With neutral Fe exponents, calculations produce no barrier, whether or not a shift in atomic orbital ionization energies to reduce charge transfer is imposed.

(h) Because of the variation in preferential ordering for binding sites as a function of cluster size, causes for the preferences will be difficult to establish using simple orbital arguments. Indeed, hybridization mixing with acetylene orbitals occurs throughout the Ni d band. The orbitals beneath the d band are slightly less stabilized for the more favored sites, whereas levels at the top are more stable for these sites. It does seem that for acetylene on Ni(111), as for O, S, Se, and Te on Ni(111), O on Fe(100), N on Cu(100), and acetylene on Pt(111) mentioned above, high coordination close packing sites are preferred, and are a consequence of balancing orbital stabilization and two-body atomic repulsion forces upon which the theoretical procedure is founded. The next theoretical step could include a search for possible coverage dependence for preferred binding sites.

Acknowledgments. Dr. J. E. Demuth aided the author in performing calculations employing 31 Ni atom clusters and

by providing stimulating comments as well as experimental results prior to their publication. Professor Earl Muetterties encouraged the analysis of bonding in the di-Ni complexes. Acknowledgment is made to the National Science Foundation and to the donors of the Petroleum Research Fund, administered by the American Chemical Society, each for partial support of this research.

References and Notes

- (1) J. E. Demuth, D. W. Jepsen, and P. M. Marcus, *Phys. Rev. Lett.*, **31**, 540 (1973).
- (2) K. O. Legg, F. P. Jona, D. W. Jepsen, and P. M. Marcus, *J. Phys. C*, **8**, 2492 (1975).
- (3) J. M. Burkstrand, G. G. Kleiman, G. G. Tibbetts, and J. C. Tracy, *J. Vac. Sci. Technol.*, **13**, 291 (1976).
- (4) L. L. Kesmodel, P. C. Stair, R. C. Baetzold, and G. A. Somorjai, *Phys. Rev. Lett.*, **36**, 1316 (1976).
- (5) R. Touroude, L. Hilaire, and F. G. Gault, *J. Catal.*, **32**, 279 (1974).
- (6) R. S. Mulliken, *Rev. Mod. Phys.*, **14**, 204 (1942); *J. Am. Chem. Soc.*, **77**, 887 (1955); A. D. Walsh, *J. Chem. Soc.*, 2260, 2266, 2288, 2296, 2301 (1953); *Prog. Stereochem.*, **1** (1954).
- (7) J. C. Robertson and C. W. Wilmson, *J. Vac. Sci. Technol.*, **9**, 901 (1972); D. J. M. Fassaert, H. Verbeek, and A. Van Der Avoird, *Surf. Sci.*, **29**, 501 (1972); L. W. Anders, R. S. Hansen, and L. S. Bartell, *J. Chem. Phys.*, **59**, 5277 (1973); A. B. Anderson and R. Hoffmann, *ibid.*, **61**, 4545 (1974).
- (8) R. C. Baetzold, *J. Catal.*, **29**, 129 (1973); *Surf. Sci.*, **36**, 123 (1973); G. Blyholder, *J. Chem. Soc., Chem. Commun.*, 625 (1973).
- (9) R. P. Messmer, C. W. Tucker, Jr., and K. H. Johnson, *Surf. Sci.*, **42**, 341 (1974).
- (10) A. B. Anderson, *Chem. Phys. Lett.*, **35**, 498 (1975).
- (11) A. B. Anderson, *J. Chem. Phys.*, **62**, 1187 (1975).
- (12) H. Hellmann, "Einführung in die Quantenchemie", Franz Neuticke and Co., Leipzig, 1937; R. P. Feynman, *Phys. Rev.*, **56**, 340 (1939).
- (13) A. B. Anderson, *J. Chem. Phys.*, **60**, 2477 (1974). Check references in this paper for applications of the Poisson equation.
- (14) R. Hoffmann, *J. Chem. Phys.*, **39**, 1397 (1963); R. Hoffmann and W. N. Lipscomb, *ibid.*, **36**, 2179 (1962); **37**, 2872 (1962).
- (15) L. Ley, S. P. Kowalczyk, F. R. McFeely, R. A. Pollak, and D. A. Shirley, *Phys. Rev. Sect. B*, **8**, 2392 (1973).
- (16) E. Clementi and D. L. Raimondi, *J. Chem. Phys.*, **38**, 2686 (1963). For usable double ζ transition metal double ζ 3d orbitals see J. W. Richardson, W. C. Nieuwpoort, R. R. Powell, and W. F. Edgell, *J. Chem. Phys.*, **36**, 1057 (1962).
- (17) W. Lotz, *J. Opt. Soc. Am.*, **60**, 206 (1970).
- (18) A. B. Anderson, *J. Chem. Phys.*, **66**, 2173 (1977); *Phys. Rev. Sect. B*, **16**, 900 (1977).
- (19) A. B. Anderson, *J. Chem. Phys.*, **65**, 1929 (1976).
- (20) Y. Wang and P. Coppens, *Inorg. Chem.*, **15**, 1122 (1976).
- (21) H. Conrad, G. Ertl, J. Küppers, and E. E. Latta, *Solid State Commun.*, 497 (1975).
- (22) C. F. Brucker and T. N. Rhodin, *Surf. Sci.*, **57**, 523 (1976).
- (23) A. B. Anderson, *Inorg. Chem.*, **15**, 2598 (1976).
- (24) F. A. Cotton, J. O. Jamerson, and B. R. Stultz, *J. Am. Chem. Soc.*, **98**, 1774 (1976); *J. Organomet. Chem.*, **94**, C53 (1975).
- (25) A. B. Anderson, *J. Chem. Phys.*, **66**, 5108 (1977).
- (26) E. L. Muetterties, W. R. Pretzer, M. G. Thomas, B. F. Beier, D. Thorn, and A. B. Anderson, to be submitted for publication.
- (27) J. E. Demuth, private communication.
- (28) G. Broden, T. Rhodin, and W. Capehart, *Surf. Sci.*, in press.
- (29) C. Kittel, "Introduction to Solid State Physics", Wiley, New York, N.Y., 1963.
- (30) L. L. Kesmodel, P. C. Stair, R. C. Baetzold, and G. A. Somorjai, *Phys. Rev. Lett.*, **36**, 1316 (1976).
- (31) G. A. Somorjai, private communication.
- (32) A. Gavezzotti and M. Simonetta, *Chem. Phys. Lett.*, **48**, 434 (1977).
- (33) T. B. Grimley, "Molecular Processes at Solid Surfaces", E. Dranglis, Ed., McGraw-Hill, New York, N.Y., 1969.
- (34) J. E. Demuth and D. E. Eastman, *Phys. Rev. Lett.*, **32**, 1123 (1974).
- (35) J. E. Demuth and D. E. Eastman, *Phys. Rev. Sect. B*, **13**, 1523 (1976).
- (36) This phenomenon is receiving attention in studies of transition metal coordination complexes by R. Hoffmann (unpublished results).
- (37) D. E. Demuth, *Chem. Phys. Lett.*, **45**, 12 (1977).
- (38) A. B. Anderson, *J. Am. Chem. Soc.*, **99**, 696 (1977).
- (39) C. F. Brucker and T. N. Rhodin, *J. Catal.*, in press.
- (40) The effects of d orbital size are entertained by C. A. Coulson, Proceedings of the Welch Foundation Conferences on Chemical Research, XVI Theoretical Chemistry, 1972.